

Banner appropriate to article type will appear here in typeset article

Spreading of a viscoelastic drop on a solid substrate

Peyman Rostami^{1,†}, Mathis Fricke², Simon Schubotz^{1,3}, Himanshu Patel¹, Reza Azizmalayeri¹, Günter K. Auernhammer[‡]

¹Leibniz-Institut für Polymerforschung Dresden e.V., Dresden, Germany,

²Department of Mathematics, TU Darmstadt, Darmstadt, Germany,

³Technische Universität Dresden, Dresden, Germany

(Received xx; revised xx; accepted xx)

We study the spreading of viscous and viscoelastic drops on solid substrates with different wettability. In the early stages of spreading, we find that the viscoelastic drop spreads faster and has a different power law than the Newtonian drop (i.e. aqueous glycerine solution) for the same zero shear rate viscosity. We argue that the effect of viscoelasticity is only observable for experimental time scales in the order of the internal relaxation time of the polymer solution or longer times. Near the contact line, the effective viscosity is lower for the viscoelastic drop than for the Newtonian drop. Together with its shear rate dependency, this difference in effective viscosity can explain the different spreading dynamics. We support our experimental findings with a simple perturbation model that qualitatively agrees with our findings.

Key words: Drop spreading, Viscoelastic liquids

1. Introduction

For at least the last two centuries, the interaction of droplets with surfaces has been studied quantitatively. In retrospective outstanding work was done by Young for static wetting (Young (1805)), Worthington for drop impact (Worthington Arthur & Reynolds (1883)) and drop spreading over different surfaces (Hardy (1919); Shuttleworth & Bailey (1948); Fox & Zisman (1950)). Drop spreading and its dynamics play an essential role in many industrial applications, from printing to coating (Hoath (2016); Sankaran & Rothstein (2012); Glasser *et al.* (2019)). The spreading of Newtonian drops has been the subject of an extensive research over the last two decades (Biance *et al.* (2004); Bonn *et al.* (2009); Bird *et al.* (2008); Snoeijer & Andreotti (2013)). For low-viscosity drops, the key finding is that the spreading dynamics consist of two regimes; an inertial and a viscous dominated regime (Biance *et al.* (2004)).

The boundary condition has an important influence on the calculation of the flow field close to the contact line and thus on the viscous dissipation. By assuming a non-slip condition, the contact line motion is solved by Moffatt (1964). The assumption of non-slip condition

[†] Email address for correspondence: rostami@ipfdd.de

[‡] Email address for correspondence: auernhammer@ipfdd.de

leads to a divergence of the viscous stress due to the hydrodynamic singularity at the moving contact line (Huh & Scriven (1971a); Tanner (1979); Huh & Scriven (1971b); Huh & Mason (1977)). Various solutions have been proposed to this problem in molecular scale (Blake & Haynes (1969)), hydrodynamic models by (Cox (1986), Voinov (1976) and Shikhmurzaev (1997, 2020)) and by including the evaporation (Rednikov & Colinet (2012)). For the fast processes, the dynamics can be modeled by the hydrodynamic model with a slip length that generates a lower cut-off length below which the liquid and solid velocities are allowed to differ in the vicinity of the contact line and/or the substrate.

Consider a drop of an initial radius R , volume of V , density ρ , viscosity η , and surface tension σ which gently touches a solid substrate, it starts spreading with velocity of u . In the early stage of spreading, inertia is assumed to be dominant (Biance *et al.* (2004)). By writing a force balance between inertial $\frac{d}{dt}((\rho V)u)$ and capillary forces $\sim \sigma r$, one can derive the spreading rate, Eq. (1.1), where the radius of the wetted on the substrate area is r .

$$\left(\frac{r}{R}\right)^2 = t \sqrt{\frac{\sigma R^3}{\rho}} \quad (1.1)$$

In a second regime, the viscous dissipation near the contact line is the rate-limiting process when the drop shape is close to a spherical cap. For the viscous dominated regime (Tanner regime) of drop spreading, the Cox-Voinov relation for the dynamic contact angle in case of perfect wetting is $\theta^3 \sim \eta \frac{u}{\sigma}$, and the conservation of volume, $r^3 \theta \sim V$, results in the spreading

dynamic in the viscous regime. This relation is known as Tanner's law $r \sim R \left(\frac{\sigma t}{\eta R}\right)^{\frac{1}{10}}$ (Tanner (1979)). It should be noted that Cox-Voinov was originally developed for a final contact angle $\theta = 0$, but was later shown to be valid for higher contact angles up to 100° (Fermigier & Jenffer (1991); Petrov *et al.* (2003)). By equating the radius from the inertial and viscous regimes, the transition between these two regimes can be calculated: $\tau_{iv} \sim \left(\frac{\rho \sigma R}{\eta^2}\right)^{\frac{1}{8}} \sqrt{\frac{\rho R^3}{\sigma}}$ (Biance *et al.* (2004)).

The above models work reasonable for low viscosity drops (e.g. water). For the early stages of high-viscosity drop spreading, there are several conflicting results (Carlson *et al.* (2011, 2012); Eddi *et al.* (2013)). Carlson *et al.* (2012) stated that the drop spreading dynamics still follow the power-law type of spreading with same exponent but with a friction factor (μ_f) as a correction factor for the prefactor of the power law, $\frac{r}{R} \sim \left(\frac{\sigma t}{R \mu_f}\right)^{\frac{1}{2}}$. Eddi *et al.* (2013) argue that, for high viscous liquids, the inviscid solution is not valid anymore, so they solve Stokes flow in this case. An important approach is to use the assumed analogy between the merging of identical drops (Eggers *et al.* (1999)) and the spreading of drops on a substrate. Eddi *et al.* (2013) used a logarithmic model to scale their experimental data $r \simeq -\frac{1}{4\pi} \frac{\sigma t}{\eta} \ln\left(\frac{t}{R}\right)$.

Despite many industrial applications (e.g. printing), the early drop spreading of viscoelastic fluids has not been extensively studied. In most of the studies, the viscous dominated drop spreading (late stage) is studied experimentally and numerically (Carré & Eustache (2000); Betelu & Fontelos (2003); Liang *et al.* (2009); Iwamatsu (2017) Jalaal *et al.* (2021); Iwamatsu (2017)). The viscous spreading exponent (α) is correlated with the rheological exponent n in these models. Just very recently, the early stage of drop spreading of shear thinning fluids is studied by two groups (Yada *et al.* (2023); Bouillant *et al.* (2022)). Both groups reported that the early stage of drop spreading (regardless of polymer concentration and molar mass) follows the same trend as low viscosity drop spreading (e.g. water drops). The considered time scale of experiments, in both cases are bellow inertia-capillary time ($\tau_{ic} = \sqrt{\frac{\rho R^3}{\sigma}}$) which is in the order of few milliseconds for millimetric drops.

Viscoelastic materials combine an elastic component and a viscous component in their properties. When a polymer solution is stretched, in the beginning only the elastic part contributes to the dynamics and after a characteristic time the viscous part becomes relevant (Costanzo *et al.* (2016)). To observe the effect of viscoelasticity, the experimental time scale should be in order of viscoelastic time scale, i.e. polymer relaxation time. In a simple approach, the viscosity of polymer solutions can be described by the Cross-model (Gastone *et al.* (2014); Subbaraman *et al.* (1971); Cross (1965)). It is shown that when shear is applied to a viscoelastic material, it takes several times of the relaxation time of the sub chain to reach a steady state. The relaxation time depends on the polymer concentration or/and molar mass (number of entanglements) (Costanzo *et al.* (2016); Vereroudakis *et al.* (2023)).

$$\eta = \frac{\eta_0 - \eta_\infty}{1 + (\tau_{ve}\dot{\gamma})^m} + \eta_\infty \quad (1.2)$$

Here $\dot{\gamma}$ is the shear rate, τ_{ve} and m are fluid parameters (polymer relaxation time and rheological exponent), and η_0 and η_∞ are zero and infinite shear rate viscosities respectively. By increasing the polymer concentration and/or polymer molar mass, the polymer relaxation time τ_{ve} increases and the rheological exponent m decreases (see SI).

In this contribution, we follow the hypothesis that three time scales should be considered; the inertia-viscous (τ_{iv}) cross over time, the inertia-capillary cross over time (τ_{ic}) and polymer relaxation time (τ_{ve}). To illustrate these time scales, we calculate them for water and an aqueous PEO solution (4% (w/w)) of the molar mass of (6×10^5 ($\frac{g}{mol}$)). For a millimetric water drop we get, $\tau_{iv} \sim 15$ ms, $\tau_{ic} \sim 3.7$ ms and $\tau_{ve} \sim 0$, and for the polymer solution $\tau_{iv} \sim 2.8$ ms, $\tau_{ic} \sim 4$ ms and $\tau_{ve} \sim 22$ ms. In this contribution, we study some effects of these changes in the order of the time scales and provide a simple model to rationalize our findings.

2. Experimental method

The droplet dispenser is set up so that the drop hangs from a needle and the substrate is lifted up gently touching the drop. After contact, the drop spreads immediately. The process is recorded in side view by a high-speed camera (FASTCAM Mini AX 200, Photron). The test section is illuminated by an LED lamp (SCHOTT KL 2500) along with a diffuser sheet to have homogeneous light in the background (Fig. 1).

Water (MicroPure UV/UF, Thermo Scientific Co.), glycerin (Sigma Aldrich co. 99%), and mixtures thereof as well as water-polyethylene oxide (PEO, Sigma Aldrich co.) solutions of various molar masses and concentrations are used as Newtonian and viscoelastic operating fluids, respectively. For aqueous PEO solution, from now on, the weight concentrations are shown as % and the molar mass of polymers are mentioned as k which represent $10^3 \frac{g}{mol}$. The sample names and viscosities at zero shear rate (zero shear viscosity) for each liquid are given in table 1. The surface tension σ of all samples is in the range of $63 \text{ mN m}^{-1} \leq \sigma \leq 72 \text{ mN m}^{-1}$. To measure the flow curves, a commercial rheometer (MRC 502, Anton-Paar GmbH) is used. For all measurements a cone-plate geometry is used with diameter of 50 (mm) and cone angle of 1° and the gap of $100 \mu\text{m}$ (CP50-1). In the rheological experiments the temperature of the sample was kept constant at $20(1)^\circ\text{C}$. The rheological properties of each sample are given in the supplementary information. Two types of surface coatings are used to study the effect of contact angle. Cleaned glass substrates as hydrophilic (contact angle of water drop around 15°) and silanised glass substrates as hydrophobic substrates (contact angle of water drop around 90°) are used. Details of substrate preparation are given in the supplementary information. When preparing polymer solutions, it is crucial to

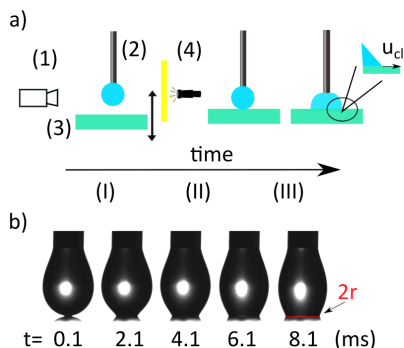


Figure 1: a) Sketch of the drop spreading setup, with high speed camera (1), light source and diffuser sheet (4), the drop and needle (2) and the adjustable solid substrate (3). Different stages of spreading are illustrated over time, (I) before contact between substrate and the drop (II) the substrate is gently coming up and the drop touches the substrate (the initial point of contact). (III) After contact and spreading of drop on the substrate with contact line velocity of u_{cl} . b) The spreading dynamics of a millimetric drop over hydrophilic substrate for different times, the spreading radius r is shown.

Sample	Molar mass ($10^3 \frac{g}{mol}$)	η_0 (mPa · s)	Sample	η_0 (mPa · s)
Water + PEO (2%, 300k)	300	35 ± 0.5	Water + Glycerin (0%)	0.93 ± 0.01
Water + PEO (3%, 300k)	300	101 ± 0.5	Water + Glycerin (72%)	35 ± 0.5
Water + PEO (4%, 300k)	300	254 ± 0.5	Water + Glycerin (85%)	98 ± 0.5
Water + PEO (2%, 600k)	600	103 ± 0.5	Water + Glycerin (91.5%)	293 ± 0.5
Water + PEO (3%, 600k)	600	537 ± 0.5	Water + Glycerin (93.5%)	389 ± 0.5
Water + PEO (4%, 600k)	600	1324 ± 0.5	Water + Glycerin (100%)	1078 ± 0.5

Table 1: Composition of operating fluids and the zero-shear viscosity η_0 (at 23 °C). The rheological properties of each sample are given in the supplementary information.

wait long enough for the polymer to dissolve homogeneously in the solution. This is illustrated by our rheology experiments. For high molar masses, we measured changes in the flow curves within the first month after preparing the sample (see supplementary information).

3. Spreading of viscoelastic and viscous Newtonian drops

3.1. Hydrophilic substrates

In Fig. 2a), we plot the radius of the wetted area (r) normalized to the initial drop radius (R), the initial spreading of viscous Newtonian (water-glycerol mixture) and viscoelastic drops on a hydrophilic substrate are plotted, (Fig. 2a). One of the experimental challenges of plotting the spreading radius over time is to determine the time of the first contact. Three options have been suggested to overcome this problem, the simplest of which is to add a bottom view camera and capture the process from bottom (Eddi *et al.* (2013)). Plotting the contact line velocity against the dimensionless spreading radius (r/R) is another possible approach (Hartmann *et al.* (2021)). The advantage of this method is that it does not need

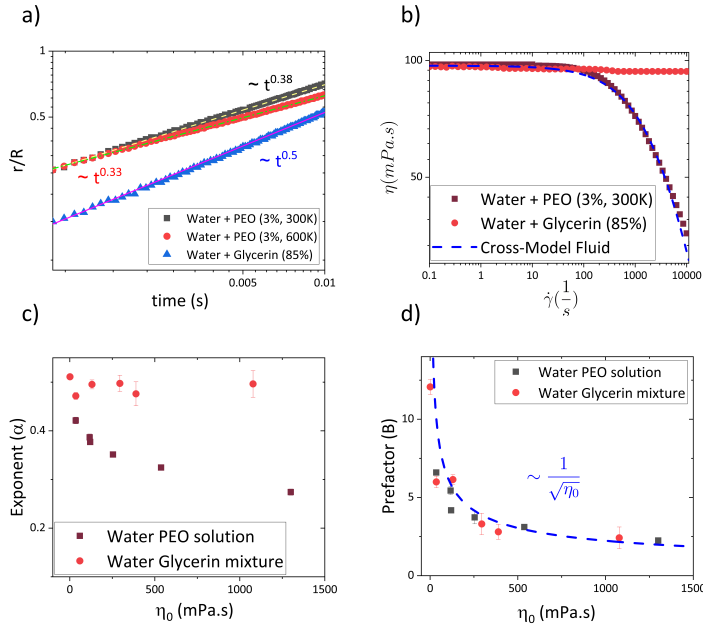


Figure 2: a) Radius of wetted area (r) normalized by initial radius of drop (R) as a function of time, for water and PEO (3%, 300k and 3%, 600k) and water and glycerin (85%) on hydrophilic substrates. b) Flow curve for water and PEO (3%, 300k) solution and mixture of water and glycerin (85%). c) and d) Spreading exponent (α) and spreading prefactor as a function of zero-shear viscosity η_0 for all viscous Newtonian and viscoelastic liquids mentioned in table 1.

the definition of zero time (see supplementary information). The third option is to define a fitting parameter as t_0 , this parameter can pop up in the fitting function $r = B(t - t_0)^\alpha$. In all our experiments, this parameter is of the order of a few frames $t_0 \sim 0.0001s$. In all plots the first four data points are omitted to be sure that the definition of the first contact time has no influence on the fit. Consequently, we fitted the drop spreading results from the fifth data point to the polymer relaxation time scale (τ_{ve}).

The viscous Newtonian drop spreads like expected from Eq. (1.1) proportional to square root of time, $r \sim \sqrt{t}$ however, aqueous PEO solutions spread with different spreading exponents ($r = B t^\alpha$). To illustrate this difference two samples with same zero-shear viscosities, here "Water + PEO (3%, 300k)" and "Water + Glycerin (85%)" ($\eta_0 \approx 100$ mPa s), same initial drop size ($D \approx 4$ mm), density, surface tension ($\sigma \approx 65$ mN m⁻¹) have clearly different spreading exponents α (Fig. 2a). Based on the present models, these drops should spread in a same manner, the major difference between two samples is the viscoelasticity of second drop. For the same prefactor in the power law, a smaller spreading exponent (α) (for $t \leq 0.01$ s) results in higher spreading rates.

To illustrate the effect of viscoelasticity, we use a typical flow curve of PEO solutions. The viscosity at low shear rates remains constant. Above a certain critical shear rate, the viscosity decays with increasing the shear rate. Such a behavior can be described by the cross-fluid model, Eq. (1.2). In contrast, water-glycerin mixtures show no evidence of shear thinning in our data, Fig. 2b. However, this may occur at even higher shear rates (Dontula *et al.* (1999)). The shear rate at which the viscosity differs from its zero shear value defines an internal relaxation time of the polymer solution, τ_{ve} in Eq. (1.2).

Our hypothesis is that the spreading dynamics depend on the rheological properties of operating fluid. The velocity of the contact line in this early regime of drop spreading is in the order of (m s^{-1}). At $1 \mu\text{m}$ from the contact line, the shear rate is estimated to be in the order of 10^6 s^{-1} . Most of the viscous dissipation occurs near the contact line (Bodziony *et al.* (2023)). At these high shear rates, the viscosity of polymer solutions decreases significantly. On the other hand, the viscosity of a Newtonian liquid remains more or less constant. This means that in the Newtonian case, the effective viscosity near the contact line is higher. Consequently, the dissipation is higher in this case, leading to a lower contact line velocity, which is in good agreement with our experimental results. This argument relies on the steady state viscosity of the liquid, i.e., when the polymer chains adapted to the shear rate and contribute to the dissipation in the polymer solution. For shorter times, the polymers cannot fully contribute to the dissipation in the polymer solution; the solution is not yet viscoelastic Costanzo *et al.* (2016); Vereroudakis *et al.* (2023).

To test our hypothesis, we measure the spreading exponent and the spreading prefactor over a wide range of zero-shear viscosities and rheological properties for viscous Newtonian and viscoelastic drops spreading on hydrophilic substrates, (Fig. 2c and d). The initial observations are verified by this systematic variation of the material parameters. For viscous Newtonian fluids, the spreading exponent is slightly decreasing with increasing zero-shear viscosity, $\alpha \approx 0.5$ on the hydrophilic substrates. In contrast, for viscoelastic fluids, the spreading exponent is a strongly decreasing function of the zero-shear viscosity, (Fig. 2c). This difference is an indication of the dependence of the spreading exponent (α) on the rheological properties. The trend of the spreading prefactor seems to depend only on the zero-shear viscosity but not on the rheological exponent (Fig. 2d). The spreading prefactor (for Newtonian and viscoelastic cases) roughly follows $B \sim \eta_0^{-0.5}$ Fig. 2d), which was also observed previously (Carlson *et al.* (2011); Eddi *et al.* (2013)).

3.2. Effect of substrate's wettability

Repeating the spreading experiments for Newtonian and viscoelastic liquids on hydrophobic substrates (i.e. $\theta_0 \simeq 90^\circ$) reveals a number of important observations, Fig. 3 a. (i) On average, the spreading exponent (α) decreases as the contact angle increases. (ii) The spreading exponent remains almost independent of zero-shear viscosity for Newtonian drops on hydrophobic substrates. (iii) Increasing the zero shear viscosity of viscoelastic liquids (i.e. increasing the concentration and/or molar mass of the polymer) reduces the exponent. The difference between the spreading of Newtonian and viscoelastic drops shows the same trend regardless of the hydrophobicity of the substrate. To summarize our experimental results, the spreading exponent is dependent on the viscoelasticity of drop and the prefactor is a function of viscosity. All of the developed models up to now cannot predict the effect of viscoelasticity, in the next section we present a simplistic model to predict this behavior.

4. Modeling

4.1. Inviscid case

For low viscosity drops, increasing the hydrophobicity of the substrate (by suitable surface modification of the substrate), results in a decreasing spreading rate and exponent (Bird *et al.* (2008); Chen *et al.* (2013); Du *et al.* (2021)). This was explained in terms of a simple energy balance. This balance assumes that no energy is dissipated. In this approximation, the kinetic energy (left hand side of Eq. 4.1) is balanced by a combination of free surface energy and

wetting energy (right hand side of Eq. 4.1, Bird *et al.* (2008)).

$$\int_V \frac{1}{2} \rho u^2 dV = \sigma [A(0) - A(t) + \pi r(t)^2 \cos(\theta_0)]. \quad (4.1)$$

Here u is the velocity field inside the drop, ρ is the liquid density, $A(t)$ and $A(0)$ are the surface area of the liquid-vapor interface during the spreading and at the time zero and θ_0 is the contact angle at which the drop spreading would stop, i.e., the static advancing contact angle. Bird *et al.* (2008) solved the balance equation (by modeling the kinetic energy integral) and showed that the spreading is a function of the substrate's wettability (Eq. 4.2).

$$r(t) = c_1 t^\alpha. \quad (4.2)$$

In this solution, the spreading exponent is $\alpha = c_2 \sqrt{F(\theta_0) + \cos(\theta_0)}$, where the unknown function F depends weakly on θ_0 (see Bird *et al.* (2008)). This means that as the contact angle increases, the spreading exponent decreases. Our experiments show the same behavior (Fig. 3 a).

4.2. Including viscous dissipation

For viscous drops, viscous dissipation cannot be neglected. The Moffatt (1964) solution suggests that the dissipation near the contact line is in the order of $\sim 2\pi\eta r u^2$. The dissipation rate is balanced by the rate of change of total energy. We add the dissipation term to the left hand side of the time derivative of Eq. 4.1. To solve the resulting equation (Eq. 4.3), we assume the viscous term to be small ($\eta \rightarrow \epsilon\eta^*$) and act as a perturbation term. From now on we drop all explicit mentioning of time as an argument.

$$2\pi\sigma \left\{ \frac{1}{2} t [\dot{r}]^2 + \frac{1}{2} t^2 [\ddot{r}] - r \dot{r} [F(\theta_0) + \cos(\theta_0)] \right\} = -2\pi\epsilon\eta^* r \dot{r}^2 \quad (4.3)$$

We rewrite Eq. 4.3 in dimensionless units ($t = \tau_{ve} \hat{t}$, $r = r^* \hat{r}$). After simplification can be rewritten as Eq. 4.4. Here the elastocapillary number is the characteristic dimensionless number $Ec = \frac{\sigma\tau_{ve}}{\eta r}$. The elastocapillary number is the ratio between the capillary time scale and the polymer relaxation time scale. In our perturbation approach, it is convenient to have Ec on the right side. We actually use the inverse of Ec , as $Ec^* = \frac{\eta^* r^*}{\sigma\tau_{ve}} = \frac{1}{Ec}$. Taking typical values for viscosity of the liquids ($\eta^* \rightarrow 100$ mPa s), the length scale as initial drop radius ($r^* \rightarrow 2$ mm) and the time scale as the highest relaxation time of polymer solution ($\tau_{ve} \rightarrow 22$ ms), we get $Ec^* \approx 0.12$.

$$\left\{ \frac{1}{2} t \dot{r}^2 + \frac{1}{2} t^2 \ddot{r} - r \dot{r} [F(\theta_0) + \cos(\theta_0)] \right\} = -\epsilon Ec^* r \dot{r}^2 \quad (4.4)$$

To address the viscoelastic case, we express the viscosity in Eq. 4.3 as $\eta \rightarrow \frac{\eta_0^*}{\dot{\gamma}^m} \rightarrow \epsilon \frac{\eta_0^*}{\dot{\gamma}^m}$. Note that $\frac{\eta_0^*}{\dot{\gamma}^m}$ has the dimensions of a viscosity. Since mainly the high shear region close to the contact line contributes to the viscous dissipation, only the high shear-rate viscosity is considered here. By estimating the shear rate as a function of the contact line velocity as $\dot{\gamma} \simeq \frac{u_{cl}}{d^*}$ (d^* is the distance to the contact line), the viscous dissipation can be written as $\simeq \eta^* r u^{2-m}$. With this assumption, the force balance equation (Eq. 4.3) can be rewritten:

$$\left\{ \frac{1}{2} t \dot{r}^2 + \frac{1}{2} t^2 \ddot{r} - r \dot{r} [F(\theta_0) + \cos(\theta_0)] \right\} = -\epsilon Ec_0^* r \dot{r}^{2-m} \quad (4.5)$$

We use Mathematica (Wolfram Alpha Co. Version 10) to solve Eq. 4.4 and 4.5 numerically,

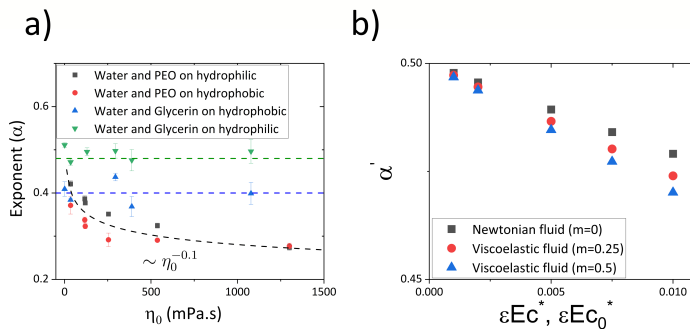


Figure 3: a) Experimental spreading exponent (α) as a function of the zero-shear viscosity η_0 for viscous Newtonian and viscoelastic liquids on hydrophobic and hydrophilic substrates. b) The theoretically predicted effective exponent (α') versus the different effective viscosity ϵEc^* values, for viscous Newtonian and viscoelastic fluids ($m = 0.25$ and $m = 0.5$).

see SI for details. We start exploring the effect of Newtonian and viscoelastic viscosity from the inviscid case discussed in (Bird *et al.* (2008)), for example we consider the case that the drop spreading follows: $r(t) = 0.02t^{0.5}$, in our dimensionless units. The obtained solution is not exactly a power law, but close to it. We fitted the numerical results by a simple power law ($B't^{\alpha'}$), where B' and α' are the effective prefactor and exponent, respectively (see SI). The theoretical exponents are plotted in Fig. 3 b as a function of ϵ and m . We consider the elastocapillary numbers are equal in both cases, since in experimental part we compare the drops with same zero shear viscosity. These results show that in viscoelastic case, the exponent decreases stronger than in the Newtonian case, by increasing the m value (i.e. increasing the viscoelasticity of samples). This agrees with the experimental observation, (Fig. 3 a). We should mention that the theoretical exponent just maps very first data points of experimental results ($\max(\eta) \rightarrow 10$ mPa s), see SI.

In summary, this simple perturbation analysis confirms the major tendencies observed in the experiments: i) Adding viscoelasticity to the system in terms of a shear-rate dependent viscosity, the effective exponent (α') decreases. ii) Increasing the viscous dissipation (i.e., the perturbation term), the prefactor decreases. This simple proposed model shows the key features of the experimental tendencies.

5. Conclusion

The early stage spreading of Newtonian and viscoelastic fluids on hydrophilic and hydrophobic substrates has been studied. Generally speaking, viscoelastic drops spread faster compared to the Newtonian case with the same physical properties (zero shear rate viscosity and surface tension). This difference can be justified by the fact that near the contact line, the shear rate is extremely high. This leads to decreasing the effective viscosity which is not the case for Newtonian liquids. To be able to observe the viscoelastic effect, the experimental time scale should be in order of internal relaxation time of the used polymer solution or longer. These experimental observations can be supported by a simple perturbation model. The results also confirm the dependency of the spreading exponent to the wettability of the substrate.

6. Funding

This study was funded by the Deutsche Forschungsgemeinschaft Project No. 265191195–SFB 1194, “Interaction between Transport and Wetting Processes” and the Deutsche Forschungsgemeinschaft (DFG) Project No. 422852551, within the priority program SPP 2171.

REFERENCES

- BETELU, SI & FONTELOS, MARCO ANTONIO 2003 Capillarity driven spreading of power-law fluids. *Applied Mathematics Letters* **16** (8), 1315–1320.
- BIANCE, ANNE-LAURE, CLANET, CHRISTOPHE & QUÉRÉ, DAVID 2004 First steps in the spreading of a liquid droplet. *Physical Review E* **69** (1), 016301.
- BIRD, JAMES C, MANDRE, SHREYAS & STONE, HOWARD A 2008 Short-time dynamics of partial wetting. *Physical review letters* **100** (23), 234501.
- BLAKE, T. D. & HAYNES, J. M. 1969 Kinetics of liquid/ liquid displacement. *J. Colloid Interf. Sci.* **30**, 421 – 423.
- BODZIONY, FRANCISCO, WÖRNER, MARTIN & MARSCHALL, HOLGER 2023 The stressful way of droplets along single-fiber strands: A computational analysis. *Physics of Fluids* **35** (1).
- BONN, DANIEL, EGGERS, JENS, INDEKEU, JOSEPH, MEUNIER, JACQUES & ROLLEY, ETIENNE 2009 Wetting and spreading. *Reviews of modern physics* **81** (2), 739.
- BOUILLANT, AMBRE, DEKKER, PIM J, HACK, MICHEL A & SNOEIJER, JACCO H 2022 Rapid viscoelastic spreading. *Physical Review Fluids* **7** (12), 123604.
- CARLSON, ANDREAS, BELLANI, GABRIELE & AMBERG, GUSTAV 2011 Measuring contact line dissipation in dynamic wetting.
- CARLSON, ANDREAS, BELLANI, GABRIELE & AMBERG, GUSTAV 2012 Universality in dynamic wetting dominated by contact-line friction. *Physical Review E* **85** (4), 045302.
- CARRÉ, ALAIN & EUSTACHE, FLORENCE 2000 Spreading kinetics of shear-thinning fluids in wetting and dewetting modes. *Langmuir* **16** (6), 2936–2941.
- CHEN, LONGQUAN, LI, CHUNLI, VAN DER VEGT, NICO FA, AUERNHAMMER, GÜNTER K & BONACCURSO, ELMAR 2013 Initial electrospreading of aqueous electrolyte drops. *Physical review letters* **110** (2), 026103.
- COSTANZO, SALVATORE, HUANG, QIAN, IANNIRUBERTO, GIOVANNI, MARRUCCI, GIUSEPPE, HASSAGER, OLE & VLASSOPOULOS, DIMITRIS 2016 Shear and extensional rheology of polystyrene melts and solutions with the same number of entanglements. *Macromolecules* **49** (10), 3925–3935.
- COX, R. G. 1986 The dynamics of the spreading of liquids on a solid surface. part 1. viscous flow. *J. Fluid Mech.* **168**, 169 – 194.
- CROSS, MALCOLM M 1965 Rheology of non-newtonian fluids: a new flow equation for pseudoplastic systems. *Journal of colloid science* **20** (5), 417–437.
- DONTULA, PRASANNARAO, MACOSKO, CHRISTOPHER W. & SCRIVEN, L. E. 1999 Does the viscosity of glycerin fall at high shear rates? *Industrial & Engineering Chemistry Research* **38** (4), 1729–1735.
- DU, JIAYU, CHAMAKOS, NIKOLAOS T, PAPATHANASIOU, ATHANASIOS G & MIN, QI 2021 Initial spreading dynamics of a liquid droplet: The effects of wettability, liquid properties, and substrate topography. *Physics of Fluids* **33** (4), 042118.
- EDDI, ANTONIN, WINKELS, KOEN G & SNOEIJER, JACCO H 2013 Short time dynamics of viscous drop spreading. *Physics of fluids* **25** (1), 013102.
- EGGERS, JENS, LISTER, JOHN R. & STONE, HOWARD A. 1999 Coalescence of liquid drops. *J. Fluid Mech.* **401**, 293 – 310.
- FERMIGIER, MARC & JENFFER, PATRICE 1991 An experimental investigation of the dynamic contact angle in liquid-liquid systems. *Journal of colloid and interface science* **146** (1), 226–241.
- FOX, HW & ZISMAN, WA 1950 The spreading of liquids on low energy surfaces. i. polytetrafluoroethylene. *Journal of Colloid Science* **5** (6), 514–531.
- GASTONE, FRANCESCA, TOSCO, TIZIANA & SETHI, RAJANDREA 2014 Green stabilization of microscale iron particles using guar gum: bulk rheology, sedimentation rate and enzymatic degradation. *Journal of colloid and interface science* **421**, 33–43.
- GLASSER, ALIZÉE, CLOUTET, ERIC, HADZIOANNOU, GEORGES & KELLAY, HAMID 2019 Tuning the rheology of conducting polymer inks for various deposition processes. *Chemistry of Materials* **31** (17), 6936–6944.

- HARDY, W BATE 1919 Iii. the spreading of fluids on glass. *The London, Edinburgh, and Dublin Philosophical Magazine and Journal of Science* **38** (223), 49–55.
- HARTMANN, MAXIMILIAN, FRICKE, MATHIS, WEIMAR, LUKAS, GRÜNDING, DIRK, MARIĆ, TOMISLAV, BOTHE, DIETER & HARDT, STEFFEN 2021 Breakup dynamics of capillary bridges on hydrophobic stripes. *International Journal of Multiphase Flow* **140**, 103582.
- HOATH, STEPHEN D 2016 *Fundamentals of inkjet printing: the science of inkjet and droplets*. John Wiley & Sons.
- HUH, C & MASON, SG 1977 The steady movement of a liquid meniscus in a capillary tube. *Journal of fluid mechanics* **81** (3), 401–419.
- HUH, CHUN & SCRIVEN, L. E. 1971a Hydrodynamic model of steady movement of a solid/liquid/fluid contact line. *Journal of Colloid and Interface Science* **35** (1), 85–101.
- HUH, CHUN & SCRIVEN, LAURENCE E 1971b Hydrodynamic model of steady movement of a solid/liquid/fluid contact line. *Journal of colloid and interface science* **35** (1), 85–101.
- IWAMATSU, MASAO 2017 Spreading law of non-newtonian power-law liquids on a spherical substrate by an energy-balance approach. *Physical Review E* **96** (1), 012803.
- JALAAL, MAZIYAR, STOEBER, BORIS & BALMFORTH, NEIL J 2021 Spreading of viscoplastic droplets. *Journal of Fluid Mechanics* **914**.
- LIANG, ZHAN-PENG, WANG, XIAO-DONG, LEE, DUU-JONG, PENG, XIAO-FENG & SU, AY 2009 Spreading dynamics of power-law fluid droplets. *Journal of Physics: Condensed Matter* **21** (46), 464117.
- MOFFATT, H. K. 1964 Viscous and resistive eddies near a sharp corner. *Journal of Fluid Mechanics* **18** (01), 1–18.
- PETROV, JORDAN G, RALSTON, JOHN, SCHNEEMILCH, MATTHEW & HAYES, ROBERT A 2003 Dynamics of partial wetting and dewetting in well-defined systems. *The Journal of Physical Chemistry B* **107** (7), 1634–1645.
- REDNIKOV, A. Y. & COLINET, P. 2012 Evaporation-driven contact angles in a pure-vapor atmosphere : the effect of vapor pressure non-uniformity. *Mathematical Modelling of Natural Phenomena* **7** (04), 53–63.
- SANKARAN, ASHWIN K. & ROTHSTEIN, JONATHAN P. 2012 Effect of viscoelasticity on liquid transfer during gravure printing. *Journal of Non-Newtonian Fluid Mechanics* **175–176**, 64–75.
- SHIKHMURZAEV, YULII D. 1997 Moving contact lines in liquid/liquid/solid systems. *J. Fluid Mech.* **334**, 211–249.
- SHIKHMURZAEV, YULII D 2020 Moving contact lines and dynamic contact angles: a ‘litmus test’ for mathematical models, accomplishments and new challenges. *The European Physical Journal Special Topics* **229** (10), 1945–1977.
- SHUTTLEWORTH, R & BAILEY, GLJ 1948 The spreading of a liquid over a rough solid. *Discussions of the Faraday Society* **3**, 16–22.
- SNOEIJER, JACCO H & ANDREOTTI, BRUNO 2013 Moving contact lines: scales, regimes, and dynamical transitions. *Annual review of fluid mechanics* **45** (1), 269–292.
- SUBBARAMAN, V, MASHELKAR, RA & ULBRECHT, J 1971 Extrapolation procedures for zero shear viscosity with a falling sphere viscometer. *Rheologica Acta* **10**, 429–433.
- TANNER, LH 1979 The spreading of silicone oil drops on horizontal surfaces. *Journal of Physics D: Applied Physics* **12** (9), 1473.
- VEREROUKAKIS, EMMANOUIL, VAN ZEE, NATHAN, MEIJER, E.W. & VLASSOPOULOS, DIMITRIS 2023 Repeated shear startup response of a supramolecular polymer. *Journal of Non-Newtonian Fluid Mechanics* **315**, 105021.
- VOINOV, O. V. 1976 Hydrodynamics of wetting. *Fluid Dynamics* **11** (5), 714–721.
- WORTHINGTON ARTHUR, MASON & REYNOLDS, OSBORNE 1883 On impact with a liquid surface. *Proceedings of the Royal Society of London* **34** (220-223), 217–230.
- YADA, SUSUMU, BAZESEFIDPAR, KAZEM, TAMMISOLA, OUTI, AMBERG, GUSTAV & BAGHERI, SHERVIN 2023 Rapid wetting of shear-thinning fluids. *Physical Review Fluids* **8** (4), 043302.
- YOUNG, THOMAS 1805 Iii. an essay on the cohesion of fluids. *Philosophical transactions of the royal society of London* (95), 65–87.